Amides. 3. Experimental and Theoretical Studies of the Effect of the Medium on the Rotational Barriers for *N*,*N*-Dimethylformamide and *N*,*N*-Dimethylacetamide

Kenneth B. Wiberg,* Paul R. Rablen, Daniel J. Rush, and Todd A. Keith

Contribution from the Department of Chemistry, Yale University, New Haven, Connecticut 06520-8107, and Lorentzian Inc., 140 Washington Avenue, North Haven, Connecticut 06473

Received January 9, 1995[⊗]

Abstract: The rotational barriers for *N*,*N*-dimethylformamide and *N*,*N*-dimethylacetamide have been investigated theoretically and experimentally. Calculations at the G2(MP2) theoretical level followed by correction to 25 °C reproduced the experimental gas-phase barriers. An examination of the geometries of these amides showed that the lower barrier for the acetamide resulted mainly from a ground state methyl−methyl repulsive interaction. The rotational barriers for the amides were measured in several solvents using NMR selective inversion−recovery experiments. The effect of solvent on the C−N rotational barriers was examined computationally using reaction field theory. This approach was found to give barriers that are in good agreement with experiment for aprotic, non-aromatic solvents which do not engage in specific interactions with the amides. The effect of a hydrogen bonding solvent, water, was studied via incorporating a water molecule hydrogen bonded to the oxygen and examining this ensemble using reaction field theory.

1. Introduction

We have examined the origin of the rotational barrier in formamide and have shown that it is largely concerned with the C−N bond and that the role of the oxygen is mainly to polarize the C−O bond so that there may be an interaction of the carbonyl carbon with the amide nitrogen.[1,2,3] We have also examined the structure of acetamide and have found that the minimum energy geometry had a rotated methyl group and a somewhat pyramidalized nitrogen, in good agreement with the structure determined via X-ray crystallography.[4] In a continuation of our study of the amide group, we wish to examine the role of the solvent in determining the magnitude of the rotational barrier.

It is known that rotational barriers for amides calculated via ab initio methods invariably are smaller than those measured experimentally.[5] A likely reason is that the calculations correspond to the gas phase while the experiments are performed almost exclusively in solution. One would expect the solvent environment to affect the barrier because of the decrease in dipole moment on going from the ground state to the rotational transition state. The ground state will then be stabilized by solvents more than the transition state leading to an increase in the barrier.[5] We were interested in seeing how well reaction field theory,[6] as incorporated into ab initio molecular orbital theory, would reproduce the observed solvent effects. A new version[7] of the Tomasi polarized continuum model (PCM)[8] has been applied to this problem.

Geometry optimizations for the amides and their rotational transition states were carried out at the MP2/6-31+G** level of theory which usually gives structures in good agreement with experimental results.[9] The diffuse functions (+) were included in order to represent the lone pairs properly.[10] Two transition states were examined where TS1 has the nitrogen lone pair anti to the carbonyl oxygen and TS2 has the lone pair syn to the oxygen. The above theoretical level is, however, often not adequate to give accurate relative energies. Therefore we have taken the optimized geometries and have calculated the energies using the G2(MP2) model,[11] which corresponds to QCISD(T)/6-311+G(3df,2p) plus correction for the zero-point energy and a higher level correction. G2(MP2) is a computationally less demanding version of the G2 model,[12] but it usually gives essentially the same relative energies as G2. These models have been shown to be quite good at reproducing experimental energies.[13]

All of the ab initio calculations were carried out using Gaussian-93.[14]

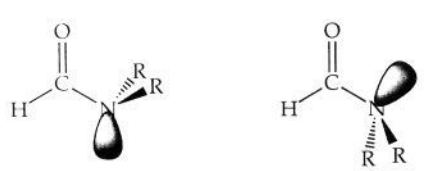

TS1 TS2

2. Gas-Phase Rotational Barriers

The rotational barriers for *N*,*N*-dimethyformamide (DMF)[15] and *N*,*N*-dimethylacetamide (DMA)[15,16] have been determined

[⊗] Abstract published in *Advance ACS Abstracts,* April 1, 1995.

(1) Wiberg, K. B.; Breneman, C. M. *J. Am. Chem. Soc.* **1992**, *114*, 831.
(2) Wiberg, K. B.; Hadad, C. M.; Rablen, P. R.; Cioslowski, J. *J. Am. Chem. Soc.* **1992**, *114*, 8644.
(3) Wiberg, K. B.; Rablen, P. R. *J. Am. Chem. Soc.* **1993**, *115*, 9234.
(4) Wong, M. W.; Wiberg, K. B. *J. Phys. Chem.* **1992**, *96*, 668.
(5) Drakenberg, T.; Dahlqvist, K. J.; Forsen, S. *J. Phys. Chem.* **1972**, *76*, 2178.
(6) Onsager, L. *J. Am. Chem. Soc.* **1936**, *58*, 1486. Cf.: Kirkwood, J. G. *J. Chem. Phys.* **1934**, *2*, 351. Born, M. *Z. Phys.* **1920**, *1*, 45.
(7) Todd, K.; Foresman, J.; Frisch, M. J.; Wiberg, K. B., to be submitted for publication.
(8) Miertus, S.; Scrocco, E.; Tomasi, J. *Chem. Phys*, **1981**, *55*, 117. Tomasi, J.; Bonaccorsi, R.; Cammi, R.; Valle, F. O. J. *J. Mol. Struct.* **1991**, *234*, 401. Tomasi, J.; Persico, M. *Chem. Rev.* **1994**, *94*, 2027.
(9) Hehre, W. J.; Radom, L.; Schleyer, P. v. R.; Pople, J. A. *Ab Initio Molecular Orbital Theory*; Wiley-Interscience: New York, 1986.
(10) Clark, T.; Chandrasekhar, J.; Spitznagel, G. W.; Schleyer, P. v. R. *J. Comput. Chem.* ***1983***, *4*, 249.
(11) Curtiss, L. A.; Raghavachari, K.; Pople, J. A. *J. Chem. Phys.* **1993**, *98*, 1293.

0002-7863/95/1517-4261$09.00/0

Table 1. Calculated Energies in Hartrees

compd	ZPE[a]	MP2[b]	DFT[b]	G2/MP2[c]	G2[c]
N,N-dimethylformamide, GS	61.83	−247.811 80	−248.533 42	−248.076 64	
N,N-dimethylformamide, TS1	61.42	−247.779 46	−248.497 30	−248.046 16	
N,N-dimethylformamide, TS2	61.18	−247.779 09	−248.497 63	−248.046 69	
N,N-dimethylacetamide, GS	78.45	−287.005 39		−287.306 73	
N,N-dimethylacetamide, TS1	78.30	−286.982 23		−287.284 26	
N,N-dimethylacetamide, TS2	77.98	−286.975 87		−287.279 63	
formamide, GS	27.65	−169.448 67		−169.640 68	−169.645 26
acetamide, GS	44.21	−208.646 12		−208.874 98	−208.880 41
ethane	44.71	−79.556 19		−79.628 93	−79.630 90
acetaldehyde	33.60	−153.402 25		−153.572 94	−153.576 81
acetone	50.41	−192.602 08		−192.808 86	−192.813 64
methylamine	38.63	−95.568 02		−95.664 51	−95.666 91
trimethylamine	72.60	−173.930 83		−174.099 89	

[a] ZPE (zero-point energy) is reported in kcal/mol at the HF/6-31G* level scaled by 0.893.[17] All amide methyl rotors and N-inversions are included anharmonically. [b] The 6-31+G** basis set was used for these optimizations. [c] The amide G2 and G2/MP2 energies include the anharmonic ZPE corrections.

Table 2. Calculation of Thermodynamic Terms for Amides, ($S°$ in cal/(mol K), All Others in kcal/mol, 25°C)

	GS				TS1				TS2			
component	$H_0^\circ - E$	$H^\circ - H_0^\circ$	S°	$G^\circ - G_0^\circ$	$H_0^\circ - E$	$H^\circ - H_0^\circ$	S°	$G^\circ - G_0^\circ$	$H_0^\circ - E$	$H^\circ - H_0^\circ$	S°	$G^\circ - G_0^\circ$
a. *N,N*-Dimethylformamide												
translation	0.0	1.48	38.78	−10.08	0.0	1.48	38.78	−10.08	0.0	1.48	38.78	−10.08
rotation	0.0	0.89	25.44	−6.70	0.0	0.89	25.35	−6.67	0.0	0.89	25.49	−6.71
vibration	61.28	0.97	4.80	−0.46	60.37	0.74	3.61	−0.33	60.18	0.74	3.58	−0.32
N-inversion	0.15	0.41	3.03	−0.50	0.37	0.31	1.73	−0.21	0.36	0.32	1.80	−0.22
Me-rotations	0.40	0.86	6.19	−0.99	0.68	0.71	4.03	−0.49	0.64	0.75	2.32	−0.54
total	61.83	4.61	78.24	−18.72	61.42	4.13	73.50	−17.78	61.18	4.18	73.97	−17.88
b. *N,N*-Dimethylacetamide												
translation	0.0	1.48	39.31	−10.24	0.0	1.48	39.31	−10.24	0.0	1.48	39.31	−10.24
rotation	0.0	0.89	26.58	−7.04	0.0	0.89	26.55	−7.03	0.0	0.89	26.59	−7.04
vibration	77.95	1.40	7.00	−0.68	77.00	1.17	5.73	−0.54	76.91	1.18	5.78	−0.54
N-inversion	0.07	0.38	3.42	−0.64	0.38	0.30	1.68	−0.20	0.32	0.36	2.11	−0.27
Me-rotations	0.43	1.17	10.11	−1.85	0.92	1.15	6.88	−0.90	0.75	1.10	7.86	−1.24
total	78.45	5.33	86.43	−20.44	78.30	5.00	80.14	−18.90	77.98	5.02	81.65	−19.32

in the gas phase. At 298 K, the activation parameters for DMF were $\Delta H^\ddagger = 19.7 \pm 0.3$ and $\Delta G^\ddagger = 19.4 \pm 0.1$, and for DMA they were $\Delta H^\ddagger = 15.8 \pm 1.1$ and $\Delta G^\ddagger = 15.3 \pm 0.1$ or 15.2 $\pm$ 0.1 kcal/mol. The $\Delta G^\ddagger$ values were calculated using a transmission coefficient of 0.5. These parameters are significantly smaller than those obtained in solution.[5] There are two interesting questions regarding these data. First, what is the reason for the difference in the rotational barrier between the two amides, and second, is it possible to reproduce the change in barrier with reaction medium via reaction field theory?

The calculated energies for the amides and their rotational transition states are given in Table 1. The G2 and G2(MP2) energies include zero point energy corrections as described below. The thermodynamic quantities for each of the compounds are given in Table 2 and the final energies corrected to 25 °C are summarized in Table 3. The $\Delta H^\ddagger$(0 K) energies correspond to the differences in G2(MP2) energies. The $\Delta H^\ddagger$(298 K) energies involve a correction for the difference in heat capacity of the ground and transition state, which depends upon the vibrational frequencies and the internal rotation modes. For consistency, the calculated frequencies were used along with a scaling factor of 0.893.[17] However, the NR_2 wag for the ground state is quite anharmonic and was treated separately as described in the Appendix. The hindered methyl rotors were treated by calculating the appropriate one-dimensional wave functions and deriving the energy levels, and this procedure is also described in the Appendix. The methyl 3-fold rotational barriers were derived from HF/6-31+G** calculations and are summarized in Table 4. The $\Delta G^\ddagger$(298 K) values were obtained in the usual fashion, except that in calculating the vibrational partition function, the methyl rotations and nitrogen inversion were again treated separately.

Table 3. Calculated Barriers for Amide Rotation (in kcal/mol) and $\Delta S^\ddagger$ (in cal/(mol K))

compd	TS	$\Delta H^\ddagger$(0K)	$\Delta H^\ddagger$(298K)	$\Delta G^\ddagger$(298K)	$\Delta S^\ddagger$(298K)
dimethylformamide	1	19.13	18.65	20.07	−4.7
	2	18.79	18.36	19.64[a]	−4.3
dimethylacetamide	1	14.10	13.77	15.64	−6.3
	2	17.01	16.70	18.13	−4.8

[a] In this case, a part of the reaction will proceed via the sightly higher energy transition state, and when this is taken into account the effective $\Delta G^\ddagger$ will be 19.4 kcal/mol.

(12) Curtiss, L. A.; Raghavachari, K.; Trucks, G. W.; Pople, J. A. *J. Chem. Phys.* **1991**, *94*, 7221. Curtiss, L. A.; Carpenter, J. E.; Raghavachari, K.; Pople, J. A. *J. Chem. Phys.* **1992**, *96*, 9030.

(13) Cf.: Curtiss, L. A.; Pople, J. A. *J. Chem. Phys.* **1991**, *95*, 7962. Curtiss, L. A.; Raghavachari, K.; Deutsch, P. W.; Pople, J. A. *J. Chem. Phys.* **1991**, *95*, 2433. Curtiss, L. A.; Brand, H.; Nocholas, J. B.; Iton, L. E. *Chem. Phys. Lett.* **1991**, *184*, 215. Ma, N. L.; Smith, B. J.; Pople, J. A.; Radom, L. *J. Am. Chem. Soc.* **1991**, *113*, 7903.

(14) Frisch, M. J.; Trucks, G. W.; Schlegel, H. B.; Gill, P. M. W.; Johnson, B. G.; Foresman, J. B.; Robb, M. A.; Cheeseman, J. R.; Keith, T.; Ayala, P. Y.; Wong, M. W.; Replogle, E. S.; Gomperts, R.; Andres, J. L.; Raghavachari, K.; Binkley, J. S.; Gonzalez, C.; Martin, R. L.; Fox, D. J.; Defrees, D. J.; Baker, J.; Stewart, J. P.; Pople, J. A. *Gaussian 93*, Development Version (Revision E.2); Gaussian, Inc.: Pittsburgh, PA, 1993.

(15) Ross, B. D.; True, N. S. *J. Am. Chem. Soc.* **1984**, *106*, 2451. Ross, B. D.; True, N. S.; Matson, G. B. *J. Phys. Chem.* **1984**, *88*, 2675. Cf.: LeMaster, C. B.; True, N. S. *J. Phys. Chem.* **1989**, *93*, 1307.

(16) Feigel, M. *J. Chem. Soc., Chem. Commun.* **1980**, 456. Feigel, M. *J. Phys. Chem.* **1983**, *87*, 3054. The $\Delta G^\ddagger$ reported therein were based on a transmission coefficient of 1.0, and it was recalculated using 0.5 to be consistent with the values given in ref 15.

(17) Pople, J. A.; Head-Gordon, M.; Fox, D. J.; Raghavachari, K.; Curtiss, L. A. *J. Chem. Phys.* **1989**, *90*, 5622. The G2 and G2/MP2 procedures use the same scaling factor.

Table 4. Calculation of Methyl Rotationl Barriers at the HF/6-31+G** Level (in kcal/mol)

	DMF			DMA		
methyl group	GS	TS1	TS2	GS	TS1	TS2
C-Me				1.5	1.8	0.4
N-Me(cis)[a]	0.8	3.6	3.2	0.4	3.6	3.2
N-Me(trans)[a]	1.9	3.6	3.2	0.4	3.6	3.2

[a] In the ground state cis and trans refer to the relationship of the methyl to oxygen.

It can be seen that the calculated C–N rotational barriers are in remarkably good agreement with the observed barriers. For DMF, the rotation is associated with transition state 2 whereas with DMA it is associated with transition state 1. As far as we are aware, this is the first calculation that has made use of a detailed treatment of rotational and NR_2 wagging modes and has reproduced the experimental gas-phase data. The calculated enthalpies of activation are not in as good agreement with the experimental values. The latter imply a small positive entropy of activation. However, it can be seen in Table 4 that the methyl rotational barriers are smaller for the ground state than the transition states. Similarly, the NR_2 wagging mode is stiffer in the transition states than in the ground state. Both of these factors along with the loss of one vibrational mode on going to the transition states require that the partition function for the ground state must increase more rapidly than for the transition states, leading to a negative entropy of activation.[18] An examination of the reported rate constants in terms of ln(k/T) vs $1/T$ shows both scatter and curvature, suggesting that the experimental $\Delta H^{\ddagger}$ may not be too reliable. The $\Delta G^{\ddagger}$ values, on the other hand, are quite reliable.

It is interesting to note that the rotational barrier for DMA is significantly smaller than that for DMF. We were interested in the origin of this difference. The following reaction would indicate whether or not it is due to a ground state energy difference:

$$H{-}CO{-}NMe_2 + CH_3{-}CO{-}NH_2 \rightarrow H{-}CO{-}NH_2 + CH_3{-}CO{-}NMe_2$$

Using the reported heats of formation, the energy change is 1.9 ± 0.8 kcal/mol,[19] and the G2(MP2) energy change (Table 1, 2.5 kcal/mol) is in good agreement. This indicates that DMA is destabilized with respect to DMF. The energy change corresponds to about 65% of the difference in the activation parameters. A similar situation is found with methyl formate and methyl acetate where the *E*/*Z* energy difference for the former is 4.5 kcal/mol and that for the latter is 8.5 kcal/mol.[20] An examination of the MP2/6-31G* structures of the compounds showed that the difference was due to a methyl–methyl steric interaction in the *E* form of methyl acetate.[21] The structures of DMF and DMA showed a similar change in bond angles, indicating that methyl–methyl steric repulsion also was present in DMA.

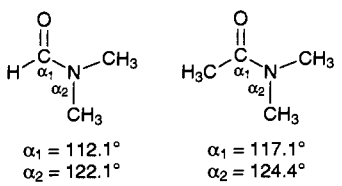

$\alpha_1 = 112.1°$ $\alpha_2 = 122.1°$ $\alpha_1 = 117.1°$ $\alpha_2 = 124.4°$

Another way of examining the interaction between methyl groups is via the use of group separation reactions (Table 5). With formamide, the energy change in the reaction with ethane is essentially the same for the parent and the *N,N*-dimethyl derivative. However, with acetamide, the reaction is significantly more endothermic with the parent than with the *N,N*-dimethyl derivative, again showing the methyl–methyl repulsive interaction. It is interesting to note the good agreement between the G2 and G2(MP2) relative energies and their agreement with the experimental data.

3. Effect of Solvent on the Rotational Barrier

The change in activation parameters on going from the gas phase to solution has been attributed to the change in dipole moment on rotation, where a polar solvent stabilizes the ground state with the higher dipole moment in preference to the transition state.[5] It also has been attributed to steric interactions in which the transition state has a greater steric requirement than the ground state, associated with the internal pressure of the solvents.[15] The latter interpretation has been questioned.[22]

Before considering theoretical approaches to calculating the rotational barriers, it is important to establish the magnitudes of the barriers in solution experimentally. Amide bond rotation in DMF and DMA has been the subject of numerous NMR bandshape fitting studies in the past.[5,23,24] Drakenberg, Dahlquist, and Forsen[5] have summarized the results of some of the more recent and reliable studies in various solvents, and Stewart and Siddall have reviewed the work prior to 1970.[25] The results, taken as a whole, clearly show that the rate of amide bond rotation decreases as either the polarity or the hydrogen bond donor ability of the solvent increases.

Although considerable data are available, they were obtained at different times by different investigators, and not in a wide enough variety of solvents for the present purposes. Therefore we have redetermined the barriers for DMF and DMA in a series of solvents chosen to represent a wide range of polarity and to include both protic and aprotic examples. In most solvents the barrier for DMA is too large to be determined at room temperature by traditional line-shape analysis, and in the past the $\Delta G^{\ddagger}$ at 25 °C has usually been extrapolated from data obtained at higher temperatures. It was possible to directly measure the rates of rotation at room temperature via NMR selective inversion–recovery experiments,[26,27] giving the data

(18) This assumes that internal rotation is adequately represented in the transition state theory model. However, if these modes were weakly coupled to the reaction coordinate and did not participate in intramolecular vibrational redistribution on a time scale shorter than the reaction time, this would not be true and could lead to an error in the calculated entropy of activation. Cf.: Kuharski, R. A.; Chandler, D.; Montgomery, J. A., Jr.; Rabii, F.; Singer, S. J. *J. Phys. Chem.* **1988**, *92*, 3261.

(19) Pedley, J. B.; Naylor, R. D.; Kirby, S. P. *Thermochemical Data of Organic Compounds*, 2nd ed.; Chapman and Hall: London, 1986. Pedley, J. B. et al. *Thermochemical Data and Structures of Organic Compounds*; Thermodynamics Research Center: College Station, TX, 1994.

(20) Blom, C. E.; Günthard, Hs. H. *Chem. Phys. Lett.* **1981**, *84*, 267.

(21) Wiberg, K. B.; Laidig, K. E. *J. Am. Chem. Soc.* **1987**, *109*, 5935.

(22) Duffy, E. M.; Severance, D. L.; Jorgensen, W. L. *J. Am. Chem. Soc.* **1992**, *114*, 7535.

(23) Rabinovitz, M.; Pines, A. *J. Chem. Soc. B* **1968**, 1110. Rabinovitz, M.; Pines, A. *J. Am. Chem. Soc.* **1969**, *91*, 1585. Neuman, R. C., Jr.; Woolfenden, W. R.; Jonas, V. *J. Phys. Chem.* **1969**, *73*, 3177.

(24) Woodbrey, J. C.; Rogers, M. T. *J. Am. Chem. Soc.* **1962**, *84*, 13. Whittaker, A. G.; Siegel, S. *J. Chem. Phys.* **1965**, *42*, 3320. Reeves, L. W.; Shaddick, R. C.; Shaw, K. N. *Can. J. Chem.* **1971**, *49*, 3683. Gutowsky, H. S.; Cheng, H. N. *J. Chem. Phys.* **1975**, *63*, 2439. Mann, B. E. *J. Magn. Reson.* **1977**, *25*, 91. Kietz, E.; Bittrich, H. J. *Z. Phys. Chem.* **1984**, *265*, 893.

(25) Stewart, W. E.; Siddall, T. H., III *Chem. Rev.* **1970**, *70*, 517.

(26) Dahlquist, F. W.; Longmuir, K. J.; DuVernet, R. B. *J. Magn. Reson.* **1975**, *17*, 406. Mann, B. E. *J. Magn. Reson.* **1976**, *21*, 17. Alger, J. R.; Prestegard, J. H. *J. Magn. Reson.* **1977**, *27*, 137. Led, J. J.; Gesmar, H. *J. Magn. Reson.* **1982**, *49*, 444. Gesmar, H.; Led, J. J. *J. Magn. Reson.* **1986**, *68*, 95. Grassi, M.; Mann, B. E.; Pickup, B. T.; Spencer, C. M. *J. Magn. Reson.* **1986**, *69*, 92. Engler, R. E.; Johnston, E. R.; Wade, C. G. *J. Magn. Reson.* **1988**, *77*, 377.

Table 5. Energy Changes for Group Separation Reactions (kcal/mol)

reaction	ΔH(0K) G2(MP2)	ΔH(0K) G2	obs(298K)
$H-CO-NH_2 + C_2H_6 \rightarrow H-CO-CH_3 + CH_3-NH_2$	20.3	20.5	21.2 ± 0.5
$H-CO-N(CH_3)_2 + C_2H_6 \rightarrow H-CO-CH_3 + (CH_3)_3N$	20.5		20.5 ± 0.5
$H_3C-CO-NH_2 + C_2H_6 \rightarrow H_3C-CO-CH_3 + CH_3-NH_2$	19.2	19.3	19.6 ± 0.3
$H_3C-CO-N(CH_3)_2 + C_2H_6 \rightarrow H_3C-CO-CH_3 + (CH_3)_3N$	16.8		16.9 ± 0.5

Table 6. Experimental Free Energies of Activation for Amide Bond Rotation (kcal/mol)[a]

solvent	ϵ[b]	$\Delta G^{\ddagger}$ for DMF[c]	$\Delta G^{\ddagger}$ for DMA[d]
gas phase	1.00	19.25[e]	15.33[f]
cyclohexane[g]	2.02 (1.98)	19.73	16.36
carbon tetrachloride	2.23 (2.18)	20.05	16.89
benzene	2.27 (2.22)	20.19	17.26
toluene	2.38 (2.32)	20.21	17.25
butyl ether	3.06	19.96	16.65
dichloromethane	9.08		17.95
acetone	20.70 (18.26)	20.45	17.49
acetonitrile	36.70 (32.70)	20.63	17.77
methanol	32.66 (27.66)	21.43	18.71
water	78.38 (69.38)	22.04	19.05

[a] Activation free energies computed from the Eyring equation by assuming a transmission coefficient of 0.5 (based on the symmetry of the isomerization). [b] Dielectric constant at 25 °C (298 K); value at 50 °C (323 K) given in parentheses if available. Source: CRC Handbook of Chemistry and Physics, 74th ed. (1993–1994); Lide, D. R., Editor in Chief; CRC Press, Inc.: Boca Raton, FL, 1993. [c] Activation energies for DMF reported for a temperature of 323.15 K. [d] Activation energies for DMA reported for a temperature of 298.15 K. [e] Gas-phase barrier for DMF obtained from the kinetic data reported in ref 15a. [f] Gas-phase barrier for DMA obtained from the kinetic data reported in ref 15b. [g] The measured rates for methyl group exchange with cyclohexane as the solvent have been raised by 3% to correct for residual concentration dependence effects—see the Experimental Section for details.

in Table 6. In the case of DMF, the rates of rotation were too slow at room temperature and were measured at 50 °C.

With structurally similar compounds one might expect the solvent effects to be related. A plot of the DMF $\Delta G^{\ddagger}$ values against the corresponding DMA values (Figure 1) was found to be linear with a slope of 0.55. The smaller effect of solvents on DMF as compared to DMA is in accord with the difference in preferred transition states for the two amides. The transition state having the nitrogen lone pair anti to the carbonyl oxygen (TS1) is clearly preferred to the syn transition state (TS2) for DMA. Since TS1 has a lower dipole moment than TS2, polar solvents reduce this preference, and in fact the Monte Carlo statistical mechanical calculations of Duffy, Severance, and Jorgensen suggest that the two transition states should be competitive in water.[22] However, in most solvents, the TS1 structure should be dominant. Table 1 shows that the case of DMF is quite different. The two possible transition states are nearly isoenergetic, with a small preference for TS2. Furthermore, as the syn transition state has the higher dipole moment, this preference increases in polar environments, and the TS2 structure should be the dominant one in all solvents. This is in accord with the QM/MM calculations of Gao.[28] Thus the solvent dependence of the DMA barriers is governed by a large dipole moment difference—that between the ground state and TS1—while the solvent dependence of the DMF barriers is governed by a relatively small dipole moment difference—that between the ground state and TS2. As a result, the solvent effect

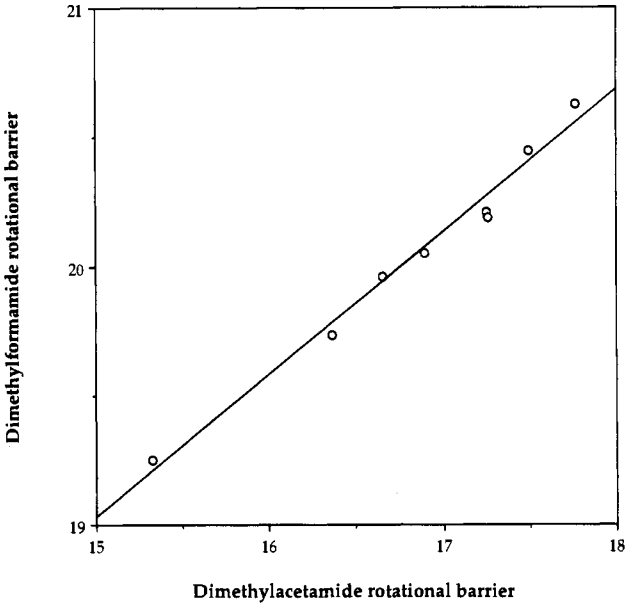

Figure 1. Relationship between the *N,N*-dimethylformamide and *N,N*-dimethylacetamide rotational barriers. The slope of the line is 0.55.

for DMA should be significantly stronger than that for DMF, as is observed in the experimental data.

The nature of the solvent effects can be seen in a plot of $\Delta G^{\ddagger}$ for DMF against the Onsager dielectric constant function, $(\epsilon - 1)/(2\epsilon + 1)$ (Figure 2). The data for the non-associating solvents cyclohexane, di-*n*-butyl ether, acetone, and acetonitrile are linearly related, and the intercept is close to the $\Delta G^{\ddagger}$ observed in the gas phase. The aromatic and halogenated solvents are known to give larger solvent effects in a variety of reactions,[29] and this phenomenon is also observed in the present case. The hydrogen bonding solvents, water and methanol, also fall off the line. The solvent dependence of *all* the barriers correlates fairly well with the empirical solvent polarity parameter E_T[30] (Figure 3). This amounts to stating that whatever property of solvents affects absorption by a typical dye chromophore also affects the amide rotational barriers in a similar fashion. This is reasonable, since both interactions will be largely determined by differences in the polarity and hydrogen bonding ability of the solutes in the ground versus their excited states. Is it possible to reproduce the experimental data using a theoretical approach?

A theoretical study of the effect of solvents on the barrier height for DMA using a Monte Carlo statistical mechanics simulation has been reported by Duffy, Severance, and Jorgensen.[22] They found that carbon tetrachloride should increase the barrier by 0.4 kcal/mol and that water should increase it by 2.1 kcal/mol. Both of the calculated energy changes are too small by ~1 kcal/mol, although the difference between carbon tetrachloride and water was well-reproduced. A study of DMF

(27) Perrin, C. L.; Thoburn, J. D.; Kresge, A. J. *J. Am. Chem. Soc.* **1992**, *114*, 8800.

(28) Gao, J. *J. Am. Chem. Soc.* **1993**, *115*, 2930. Gao, J. *Proc. Indian Acad. Sci.* **1994**, *106*, 507.

(29) Abraham, R. J.; Brentschneider, E. In *Internal Rotation in Molecules*; Orville-Thomas, W., Ed.; Wiley: London, 1974; Chapter 13. Wiberg, K. B. Physical Organic Chemistry; Wiley: NewYork, 1965; p 384–5.

(30) Reichardt, C. *Solvent Effects in Organic Chemistry*; Verlag Chemie: Weinheim, 1979.

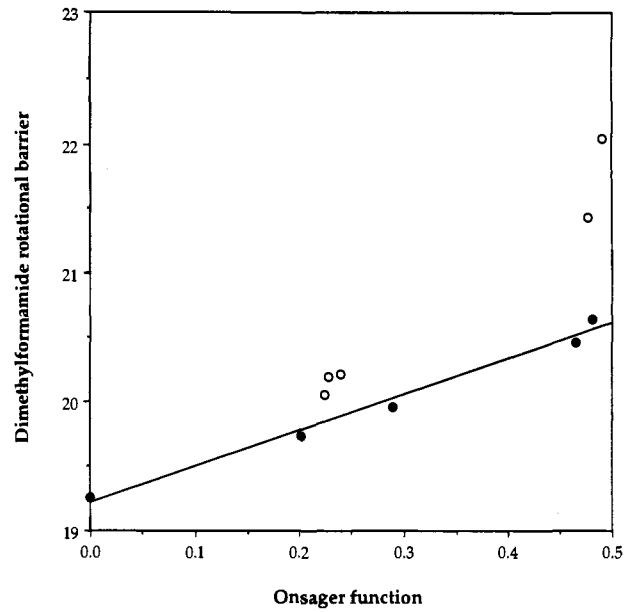

Figure 2. Relationship between the observed *N,N*-dimethylformamide rotational barriers and the Onsager function $(\epsilon - 1)/(2\epsilon + 1)$. The solid circles from left to right correspond to the gas phase, cyclohexane, di-*n*-butyl ether, acetone, and acetonitrile. The group of open circles in the middle correspond to carbon tetrachloride, benzene, and toluene. The open circles at the right correspond to the hydrogen bonding solvents—methanol and water.

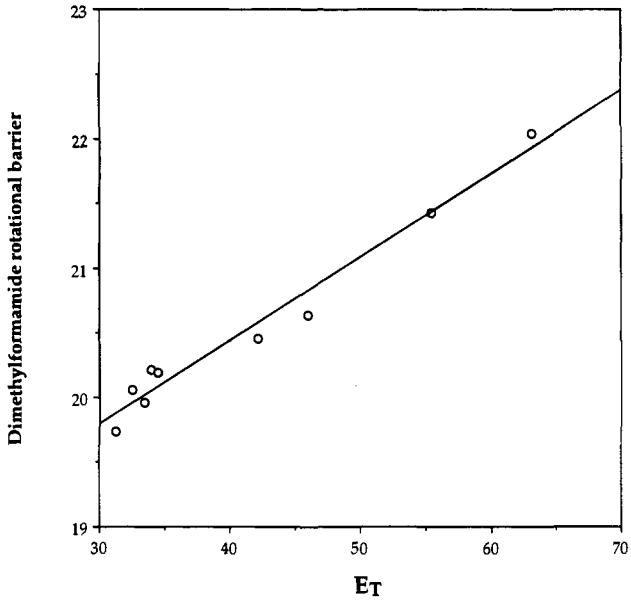

Figure 3. Relationship between the observed dimethylformamide rotational barriers and the Dimroth–Reichardt solvent polarity parameter, E_T.

has been reported by Gao[28] that predicted a barrier in water of 20.8 kcal/mol, significantly smaller than the observed barrier (22.4 kcal/mol).

We wished to see if the reaction field model[7] would reproduce the change in barrier on going from the gas phase to solution. In this model, the solute is placed in a cavity in the solvent, and the latter is taken as an unstructured dielectric continuum. The simplest reaction field model uses a spherical cavity and considers only the dipole moment of the solute.[31] This moment leads to a reflection moment in the solvent that is aligned to give attractive interactions and leads to stabilization. The magnitude of the reflection moments determined by the solvent dielectric constant. This model is limited to fairly compact molecules for which the dipole is the dominant electric moment.

In order to have a more realistic cavity shape and more adequately treat the charge distribution in the solute, Rivail and Rinaldi developed a model that uses an ellipsoidal cavity and considers the solute's electric moments up to the sixth order.[32] An ellipsoidal cavity is still not a good approximation to the shape of many molecules, and in some cases even the use of the sixth-order moment is not a sufficiently good approximation to infinite order.[7] Tomasi has developed a polarized continuum model (PCM) that describes the solute in terms of a set of interlocking spheres having slightly enlarged van der Waals radii and calculates surface potentials for a selected number of points.[8] The solvent effect is derived from the interactions of the surface potentials with the dielectric continuum. This procedure is equivalent to going to infinite order in the electric moments.

We have developed a modified version of this model (IPCM, isodensity polarizable continuum model) that defines the cavity in terms of a surface of constant charge density for the solute.[7] It has been found that a value of 0.0004 e/B^3 yields volumes that are very close to the observed molar volumes. In this method, besides the choice of theoretical level, there are only two parameters: the solvent dielectric constant and the charge density to be used in defining the surface. For any given problem, both are fixed by experimental data, and so there are no adjustable parameters. This model has been applied to the calculation of solvent effects on the amide rotational barriers.

At the present time, the IPCM model is able to calculate solvent effects and to permit geometry optimizations in the presence of a solvent for RHF and density functional theory (DFT) methods, but not for MP2. With the latter, it is possible to calculate solvent effects, but it is not as yet possible to carry out geometry optimizations efficiently. DFT often leads to results comparable to MP2, and therefore geometry optimizations have been carried out at the DFT/6-31+G** theoretical level for DMF and its rotational transition states (Table 1).[33] However, the gas-phase rotational barriers calculated at this level of theory were too large by about 3 kcal/mol, and it was not further considered.

Although one might expect some structural changes to accompany the change from the gas phase to solution, they would not be expected to have a large effect on the calculated energy changes.[32] RHF/6-31+G* geometry optimizations for formamide with $\epsilon = 36$ found no significant change in relative energies as compared to the use of gas-phase geometries. Therefore, all of the solvent effect calculations were carried out using the gas-phase MP2/6-31+G** geometries. Both the RHF/6-31+G* and MP2(fc)/6-31+G* theoretical levels were used, giving the results summarized in Table 7. The energy differences are given in Table 8. It can be seen that solvent effects calculated at the RHF and MP2 levels are somewhat different. The latter gives the better description of the charge distribution,

(31) Cf.: Wong, M. W.; Frisch, M. J.; Wiberg, K. B. *J. Am. Chem. Soc.* **1991**, *113*, 4776. Wong, M. W.; Wiberg, K. B.; Frisch, M. J. *J. Chem. Phys.* **1991**, *95*, 8991.

(32) Rinaldi, D.; Ruiz-Lopez, M. F.; Rivail, J.-L. *J. Chem. Phys.* **1983**, *78*, 834. Rinaldi, D.; Rivail, J.-L.; Rguini, N. *J. Comput. Chem.* **1992**, *13*, 675.

(33) Stephens, P. J.; Devlin, F. J.; Chabalowski, C. F.; Frisch, M. J. *J. Phys. Chem.* **1994**, *98*, 11623. Here $E_{xc}^{Becke3LYP} = A^* E_x^{LSD} + (1 - A)^* E_x^{HF} + B^* \Delta E_x^{B88}$ $C^* E_c^{LYP} + (1 - C)^* E_c^{VWN}$, where $A = 0.8$, $B = 0.72$, and $C = 0.81$. The Becke3LYP functional, as implemented in Gaussian, uses the values of *A*, *B* and C suggested by Becke (Becke, A. D. *J. Chem. Phys.* **1993**, *98*, 5648) but uses the LYP (Lee, C.; Yang, W.; Parr, R. G. *Phys. Rev. B* **1988**, *37*, 785) correlation functional and the VWN (Vosko, S. H.; Wilk, L.; Nusair, M. *Can. J. Phys.* **1980**, *58*, 1200) local correlation expression rather than the Perdew–Wang (Perdew, J. P. In *Electronic Structures of Solids*; Ziesche, P., Eschrig, H., Eds.; Akademie Verlag: Berlin, 1991) gradient correction for correlation.

Table 7. Calculated Solvent Effect for Amide Rotation[a]

compd	ϵ	RHF/6-31+G*	μ	MP2(fc)/6-31+G*	μ
DMF, GS	1	−246.995 24	4.594	−247.733 68	4.359
	2	−246.999 85	5.049	−247.737 27	4.845
	3	−247.001 87	5.249		
	5	−247.003 73	5.435	−247.740 40	5.266
	10	−247.005 31	5.593		
	80	−247.006 85	5.747	−247.742 96	5.611
DMF, TS1	1	−246.964 59	2.224	−247.701 86	1.762
	2	−246.967 46	2.435	−247.703 80	1.927
	3	−246.968 74	2.529		
	5	−246.969 93	2.616	−247.705 47	2.066
	10	−246.970 95	2.691		
	80	−246.971 95	2.765	−247.706 84	2.177
DMF, TS2	1	−246.963 37	4.161	−247.701 48	3.600
	2	−246.967 44	4.564	−247.704 30	3.969
	3	−246.969 26	4.745		
	5	−246.970 98	4.916	−247.706 82	4.297
	10	−246.972 46	5.065		
	80	−246.973 94	5.213	−247.708 96	4.576
DMA, GS	1	−286.034 50	4.366	−286.906 03	4.082
	2	−286.038 82	4.837	−286.909 38	4.563
	3	−286.040 74	5.046		
	5	−286.042 54	5.248	−286.912 37	4.998
	10	−286.044 09	5.423		
	80	−286.045 60	5.597	−286.914 88	5.368
DMA, TS1	1	−286.012 61	2.332	−286.883 32	1.879
	2	−286.015 56	2.585	−286.885 35	2.082
	3	−286.016 87	2.699		
	5	−286.018 11	2.807	−286.887 13	2.259
	10	−286.019 17	2.901		
	80	−286.020 22	2.994	−286.888 62	2.405
DMA, TS2	1	−286.005 74	4.305	−286.876 74	3.775
	2	−286.010 11	4.765	−286.879 92	4.208
	3	−286.012 08	4.977		
	5	−286.013 95	5.181	−286.882 80	4.603
	10	−286.015 58	5.359		
	80	−286.017 20	5.539	−286.885 29	4.949

[a] Energies are given in hartrees, dipole moments in debye.

Table 8. Calculated Energy Changes for Rotation in Solutions[a]

	RHF		MP2	
ϵ	TS1	TS2	TS1	TS2
	a. *N,N*-Dimethylformamide			
1	19.23	20.00	19.97	20.21
2	20.33	20.34	21.00	20.69
3	20.79	20.46		
5	21.21	20.55	21.92	21.07
10	21.56	20.61		
80	21.90	20.65	22.67	21.34
	b. *N,N*-Dimethylacetamide			
1	13.74	18.05	14.25	18.38
2	14.60	18.02	15.08	18.49
3	14.98	17.98		
5	15.33	17.94	15.84	18.56
10	15.64	17.89		
80	15.93	17.82	16.48	18.57

[a] These data correspond to 0 K and are not corrected for zero-point energy differences.

and therefore should be the more reliable. The MP2 values will be used in the following discussion.

In order to relate the calculated solvent effects to the experimental data, we have proceeded as follows. The G2-(MP2) energy difference was used for the gas phase. Dipole and higher electric moments do not change much on going from MP2 to higher correlated levels of theory, and therefore the changes in energy calculated at the MP2 level were combined with the G2(MP2) energies to give the estimates of the barrier heights in solution at 0 K. These data were then converted to free energies at 298 K as described above, and the final values are given in Table 9.

Table 9. Calculated Rotational Barriers in Solution ($\Delta G^{\ddagger}$(298K) in kcal/mol)

	DMF			DMA		
ϵ	TS1	TS2	combined[a]	TS1	TS2	combined[a]
1	20.07	19.64	19.41	15.64	18.13	15.63
2	21.11	20.12	20.02	16.47	18.24	16.44
5	22.02	20.51	20.46	17.23	18.31	17.14
80	22.77	20.77	20.75	17.87	18.32	17.64

[a] Adjusted to take into account the part of the reaction that proceeds via the higher energy transition state.

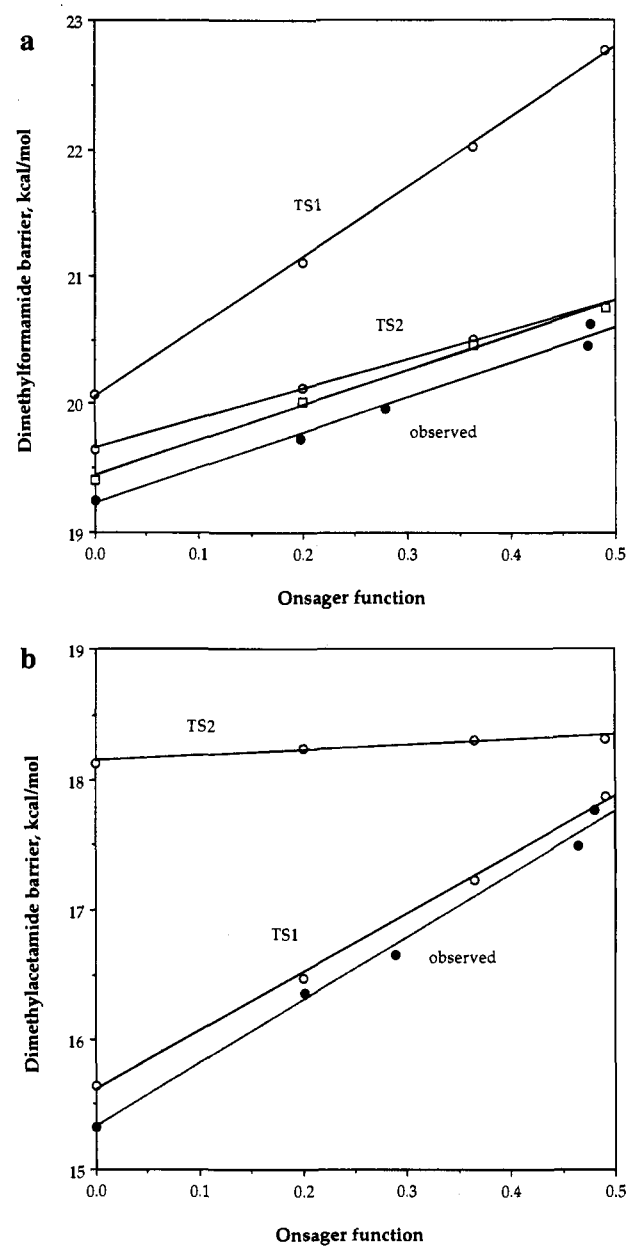

Figure 4. Comparison of calculated and observed solvent effects on the rotational barriers for (a) *N,N*-dimethylformamide and (b) *N,N*-dimethylacetamide. The calculated barriers are shown as open circles and the observed barries are given as closed cirlces. With DMF, the calculated $\Delta G^{\ddagger}$ values based on both TS1 and TS2 (combined column in Table 9) are given as open squares.

In order to compare the calculated and observed solvent effects, the $\Delta G^{\ddagger}$ values have been plotted against the corresponding values of the Onsager function in Figure 4. In the case of DMF the difference in energy between the two transition states is fairly small, and both reaction channels will be operative. The net $\Delta G^{\ddagger}$ for the process is given as $\Delta G^{\ddagger}$-

Table 10. Effect of Hydrogen Bonding on DMF, HF/6-31+G* [a]

state	TS2	GS	ΔE (kcal/mol)
DMF, $\epsilon = 1$	−246.966 45 (3.888)	−246.997 73 (4.504)	19.63
DMF + H_2O, $\epsilon = 1$	−322.992 05 (2.865)	−323.025 97 (4.880)	21.28
DMF + H_2O, $\epsilon = 80$	−323.005 85 (3.358)	−323.040 46 (5.605)	21.72

[a] Total energies are given in hartrees and the dipole moments are given in parentheses in debye.

(combined). With both DMF and DMA the calculated energy differences are very close to the observed differences. It is fair to say that the reaction field model is quite successful in reproducing the data for the gas phase and for this set of solvents (cyclohexane, di-*n*-butyl ether, acetone, and acetonitrile).

4. Hydrogen Bonding Effects

Reaction field theory is appropriate only for solvents that do not give specific interactions, such as hydrogen bonding, with the solute. Thus, it is not surprising that the effect of water as the solvent is not well-reproduced. One way in which to minimize this problem is to add one or more water molecules to the solute, and then calculate the energy of this ensemble via reaction field theory.[34] We have carried out a preliminary application of this method to the rotational barrier for DMF (Table 10).

It was found that the principal hydrogen bonding site was the carbonyl oxygen.[22,28] The structures of the ground state and TS2 plus one water molecule were obtained at the RHF/6-31+G* level of theory. It was found that hydrogen bonding in the gas phase increased the rotational barrier by 1.65 kcal/mol. When these complexes were placed in a medium with $\epsilon = 80$, the barrier increased by an additional 0.44 kcal/mol, giving a net increase of 2.1 kcal/mol. This is in reasonable agreement with the observed increase of 2.8 kcal/mol and indicates that this approach is worth further study. A more detailed examination of this question will require the inclusion of hydrogen bonding at nitrogen, and this is in progress.

5. Conclusions

The effect of solvent on the barrier to C−N bond rotation in amides has been studied experimentally via NMR spectroscopy and theoretically via ab initio MO calculations. In agreement with previous reports, the barriers were observed to increase in polar solvents, as a result of the greater stabilization of the more polar ground state as compared to the less polar transition states. The effect was greater with *N,N*-dimethylacetamide than with *N,N*-dimethylformamide because of a qualitative difference in the transition states. The former prefers a structure having the nitrogen lone pair anti to the carbonyl oxygen resulting in a fairly small dipole moment, while the latter prefers a structure with the nitrogen lone pair syn to the carbonyl oxygen, resulting in a relatively large dipole moment. Since the ground state has a large dipole moment, the difference in solvation between the ground state and the transition state is greater with DMA than with DMF, leading to the greater solvent effect.

Calculations at the G2/MP2 level, after correction to give $\Delta G^{\ddagger}$ at 298K, reproduced the gas-phase experimental free energies of activation for C−N bond rotation in DMF and DMA. The new self-consistent reaction field (SCRF) model (IPCM) has been found to reproduce the medium effects for both amides in solvents that do not give special interactions with the amides, such as cyclohexane, di-*n*-butyl ether, acetone, and acetonitrile. The barriers in these solvents and the gas phase are well correlated with the Onsager dielectric constant function $(\epsilon - 1)/(2\epsilon + 1)$. The barriers in aromatic and chlorinated solvents (benzene, toluene, dichloromethane, and carbon tetrachloride) were somewhat higher than predicted by the continuum model, probably due to their higher than average polarizabilities.

The hydrogen bonding solvents, water and methanol, further raise the barriers by ~0.5−1.0 kcal/mol as compared to the polar aprotic solvents. The effect of water was fairly well-reproduced using a simple model having one explicit water molecule associated with the amide and using the reaction field model to represent the rest of the solvent.

Self-consistent reaction field theory provides a useful and computationally efficient model for the study of solvent effects. It provides a base line for the effect of non-interacting solvents for both equilibria and rates of reaction. Deviations from the predictions of solvent effects provide a measure of special solvent interactions, such as those due to higher than average polarizabilities (as seen in the corresponding refractive indices) or hydrogen bonding. The SCRF model does reproduce the significant effect of relatively nonpolar solvents such as cyclohexane on both rates of reaction and equilibria whereas most fluid simulation models predict very small effects for these solvents. The latter models usually do not include terms for the polarizability of the solvent, and therefore do not reproduce dipole−induced dipole interactions. The latter are included in the SCRF models through the dielectric constant.

6. Experimental Section

Sample Preparation. DMF and DMA were obtained from Aldrich and distilled under vacuum prior to use. Deuterated solvents were obtained from Aldrich (most cases), Janssen Chimica (toluene), and Cambridge Isotope Laboratories (butyl ether). Carbon tetrachloride was obtained from Baker. Carbon tetrachloride and deuterated benzene, toluene, cyclohexane, acetone, acetonitrile, and dichloromethane were treated with 4 Å molecular sieves and BaO prior to use. Deuterated water and methanol were used as received. NMR samples were prepared by placing 2 μL of DMF or DMA in 1.0 mL of the appropriate solvent in an NMR tube. The solution was then cooled in liquid nitrogen (most cases), dry ice−acetone (CD_3OD and CD_2Cl_2), or cold water (D_2O) and the tube was subjected to vacuum and sealed.

Calibration of the Variable-Temperature NMR Probe. All NMR experiments were carried out using a General Electric Ω-300 (300 MHz) spectrometer operated by a Sun workstation and equipped with a variable-temperature 5-mm broad-band probe (300/44 5MM 31P-15N/H). The calibration of the probe's temperature controller was established at least once per week against a vacuum-sealed methanol standard. The difference in chemical shifts for the two methanol peaks was measured at a series of ~8 temperatures separated by ~10° intervals, and the corresponding temperatures were calculated from the equation below in which $\Delta\delta$ is the chemical shift difference in ppm.[35] The calibrated temperature was calculated as the average of ten

$$T(\mathrm{K}) = 409.0 - 36.54(\Delta\delta) - 21.85(\Delta\delta)^2$$

determinations made over a 10-min period after an hour of temperature equilibration time. Selective inversion−recovery experiments were not carried out at a given temperature unless that temperature had been calibrated some time within the previous week. In general, the calibrated temperature corresponding to a given temperature setting did not vary by more than ±0.5° from one week to the next. Variability

(34) Tortonada, F. R.; Pascual-Ahuir, J.-L.; Silla, E.; Tuñón, I. *J. Phys. Chem.* **1993**, *97*, 11087. Tuñón, I.; Silla, E.; Bertrán, J. *J. Phys. Chem.* **1993**, *97*, 5547.

(35) Ammann, C.; Meier, P.; Merbach, A. E. *J. Magn. Reson.* **1982**, *46*, 319.

was even lower for temperatures near room temperature, but occasionally somewhat greater (~±1.0°) for temperatures far above or below room temperature. For experiments below room temperature, nitrogen gas entering the probe was pre-cooled a 2-propanol bath cooled by either an electrical chiller (for experiments between 20 and −15 °C) or dry ice (for experiments below −15°). For experiments at and above room temperature, air was used to maintain temperature control. Temperature calibration was always performed under the same temperature control conditions as the experiments for which the calibration was used, i.e., for experiments using a dry ice−2-propanol bath, the calibration was also performed with dry ice−2-propanol, for experiments using 2-propanol cooled by the electrical chiller, the calibration was also performed using the electrical chiller, etc.

Selective Inversion−Recovery Experiments. Selective inversion−recovery (SIR) experiments were then carried out in the standard fashion,[26,27] except that an automated c-shell script (available upon request: e-mail to rablen%kbwgpx@biomed.med.yale.edu) was used to run the experiments without user intervention. The standard SIR pulse sequence shown below was programmed into the system (with a 4-step phase cycle), where t_{ev} is the evolution time and t_{mix} is the mixing time.

$$90°_x \rightarrow t_{ev} \rightarrow 90°_y \rightarrow t_{mix} \rightarrow 90°_x \rightarrow \text{observe (FID)}$$

For the experiment to work properly, the offset frequency is set to exactly halfway between the two exchanging methyl peaks, and the evolution time is set to one-half the reciprocal of the difference in the two peak positions in hertz. The mixing time then should take on a series of values corresponding to roughly 5 halflives for the exchange process. Typically, 10−15 different mixing times were used for each rate measurement, and 4 scans were taken for each spectrum. A delay between pulses of 130 s was used to ensure complete relaxation and avoid the artifacts which incomplete relaxation might cause. At least an hour was allowed for the temperature to equilibrate at a new value before any experiment was carried out.

The integrated peak intensities for a given series of mixing times were then fit to the equation below in a least-squares sense.[36]

$$\ln\left(\frac{(M_0 - M_{za}(t)) - (M_0 - M_{zx}(t))}{(M_0 - M_{za}(t)) + (M_0 - M_{zx}(t))}\right) = -2k_r t$$

M_0 refers to the equilibrium magnetization (intensity), $M_{za}(t)$ the magnetization of peak A at mixing time t, $M_{zx}(t)$ the magnetization of peak X at mixing time t, and k_r the rate constant for exchange. The fitting was accomplished using a FORTRAN program written to interface with the c-shell script which runs the SIR experiments, and it is available upon request. These equations assume equal t_1 relaxation times for the two methyl peaks and make some other assumptions as well. However, as long as exchange is fairly rapid compared to longitudinal relaxation, whether or not this assumption is correct will make almost no difference for the computed rate constant. Perrin has used a much more sophisticated equation, having seven adjustable parameters and making fewer assumptions, to model his SIR data.[27] However, we have chosen the simple equations above in the hopes that, with only two adjustable parameters, any serious problems with the data would show up as a nonlinear plot. In actual fact, an extremely high degree of linearity was obtained, with r^2 values typically 0.995 or better, and almost never below 0.99, although in some cases with slow exchange only 2 or 3 halflives could be used. Any experiment with $r^2 < 0.98$ for ~3 halflives was rejected.

For each compound (DMA and DMF) and solvent, experiments were performed at a series of ~5 temperatures around 25 °C (DMA) or 50 °C (DMF) separated by ~10° intervals. The value of $\Delta G^‡$ at 25 °C (DMA) or 50 °C (DMF) was then obtained by fitting the data points to the Eyring equation with the transmission coefficient set to 0.5. These values, which in a sense represent an average, are reported in Table 6. The individual experimental rate constants are tabulated in the supplementary material.

(36) Harris, R. K. *Nuclear Magnetic Resonance Spectroscopy*; John Wiley & Sons: New York, New York 1987; p 172.

The rates of methyl group exchange in DMF and DMA are known to be concentration dependent in nonpolar solvents, presumably due to association between the molecules.[23a] This difficulty plagued many of the early studies of C−N bond rotation in amides, since the NMR spectrometers available at the time did not have the sensitivity necessary for working with highly dilute samples. With the benefit of a modern 300-MHz FT spectrometer, however, we were able to perform all experiments at or near the low concentration limit. With concentrations of 0.2% by volume, the rate constants appeared to be within ~3% of their limiting value even in cyclohexane, the least polar solvent studied, and within ~2% or better for all the other solvents. The rate constants reported in cyclohexane have been raised by 3% to account for this factor, which results in a lowering of the reported barrier by 0.02 kcal/mol. The full details of the concentration dependence study will be published separately.

As a check on the rates of rotation determined in this fashion, the more common complete band shape fitting procedure (CBS) also was used in several cases. With DMA in benzene at 44.6 °C, the $\Delta G^‡$ values were 17.26 (SIR) and 17.17 (CBS) kcal/mol, and in acetonitrile at the same temperature they were 17.74 (SIR) and 17.68 (CBS) kcal/mol. The agreement between the two methods was excellent.

Error Estimates. The error in rate constants determined in these experiments is estimated at ±5%, and the uncertainty in the temperature at ±0.5° (based on the variability of the weekly temperature calibrations), leading to an overall uncertainty of ±8% for the rate data and of ±0.05 kcal/mol for $\Delta G^‡$ in the vicinity of room temperature. The uncertainty is likely somewhat greater (±0.10 kcal/mol) for experiments significantly above or below room temperature due to a greater variability in the temperature control. Thus the $\Delta G^‡$ values have an uncertainty of ±0.05 kcal/mol for DMA (reported at 25 °C) and ±0.10 kcal/mol for DMF (reported at 50 °C).

Appendix: Thermodynamic Corrections for Methyl Rotors and Nitrogen Inversion

General. The partition function for a molecule must be calculated in order to compute thermodynamic quantities such as enthalpy, entropy, and free energy at temperatures above absolute zero from ab initio calculations. The partition function is generally separated into translational, rotational, and vibrational components. The first two can be treated in a fashion which is rigorous for all reasonable temperatures.[37]

$$Q_{trans} = \left(\frac{2\pi mkT}{h^2}\right)^{3/2}\left(\frac{NkT}{P}\right)$$

$$Q_{rot} = \left(\frac{8\pi^2 kT}{h^2}\right)^{3/2} \pi^{1/2}(I_A I_B I_C)^{1/2}\,\sigma^{-1} \quad \text{(nonlinear molecules)}$$

If the modes are harmonic, the vibrational component can also be treated simply, by summing over the normal modes of the molecule as shown in the equation below. The values of ω_i are the harmonic frequencies.

$$Q_{vib} = \prod_i^{3n-6}(1 - e^{-hc\omega_i/kT})^{-1}$$

However, if one or more modes are not well-described by a harmonic oscillator potential function, a more appropriate approximation is required. Usually the low-frequency modes are the ones least well represented by a harmonic oscillator. Thus the effects on the zero-point energy and the enthalpy are generally small, but the effects on the entropy, and thus the free energy, can be substantial. In DMF and DMA, the methyl rotors and the nitrogen inversion mode are the most important cases in which the harmonic oscillator approximation is poor.

(37) Janz, G. J. *Thermodynamic Properties of Organic Compounds: Estimation Methods, Principles and Practice*, revised edition; Academic Press: New York, 1967.

The product in the equation above was obtained while excluding these modes, for which the contributions to the thermodynamic properties were calculated separately. We make the assumption that all modes are uncoupled and calculate the contribution of each to the enthalpy and entropy using the formulas below.[38]

$$H_T^\circ - H_0^\circ = \frac{N_A \sum_{n=0}^{\infty} \epsilon_n e^{-\epsilon_n/kT}}{\sum_{n=0}^{\infty} e^{-\epsilon_n/kT}}$$

$$S^\circ = \frac{H_T^\circ - H_0^\circ}{T} + N_A k \ln\left(\sum_{n=0}^{\infty} e^{-\epsilon_n/kT}\right)$$

Here ϵ_n are the energy levels referenced to the zero-point energy (i.e., $\epsilon_0 = 0.0$).

Methyl Rotors. The partition function for the methyl rotors was obtained by using a sinusoidal potential function of the form shown below, where V_0 is the barrier height.

$$V(\theta) = \frac{1}{2} V_0(1 - \cos(3\theta))$$

This functional form provides a 3-fold symmetric potential which must be close to the true functional form, yet is easy to parametrize and calculate. The partition function is calculated from the quantized energy levels of the hindered rotor, which are the solutions to the one-dimensional time-independent Schrödinger equation for circular motion (rotation about a single axis) with this potential energy function.

$$\frac{-\hbar^2}{2I_r}\frac{d^2\psi(\theta)}{d\theta^2} + [V(\theta) - E]\psi(\theta) = 0$$

The energy levels were obtained variationally as the eigenvalues of the appropriate matrix[38] using the free (unhindered) rigid rotor wave functions as a basis set (these are the solutions to the classical "particle on a ring" problem).[39] A FORTRAN program was written to solve the eigenvalue problem numerically using a standard subroutine implementing the Jacobi method.[40] Convergence of the first twenty energy levels to ± 1 μhartree was requested of the calculations, which typically required ~100 basis functions. The reduced moment of inertia for the methyl group was taken to be 5.303×10^{-40} g·cm^2 in all cases, a standard value which should serve with sufficient accuracy for the present purposes.[37]

Pitzer and Gwinn addressed the problem of the partition function for hindered rotors many years ago and developed a series of tables from which enthalpies, entropies, and free energies can be interpolated.[41] As a comparison, thermodynamic properties for the methyl rotors were derived from these tables, using the same reduced moment of inertia and barrier heights as with the calculations above. Essentially identical numerical results were obtained.

Nitrogen Inversion. Insufficient experimental data exist to obtain literature values for the DMF and DMA inversion energy levels. The alternative is to calculate these properties ab initio. Similar to hindered methyl rotors, energy levels for the amide inversion mode are solutions to the one-dimensional time-independent Schrödinger equation below.[39]

$$-\frac{\hbar^2}{2\mu}\frac{d^2\psi(q)}{dq^2} + [V(q) - E]\psi(q) = 0$$

Here q is the inversion coordinate, μ is the reduced mass appropriate for q, and V(q) is an analytical form of the inversion potential function.

For each molecule a **Z**-matrix was constructed in such a way that an imaginary atom maintained equal angles between itself, nitrogen, and the three nitrogen substituents. We chose to describe q as the amount of pyramidalization occurring at the nitrogen atom ($q = \angle$XNR $- 90°$). This allowed a full range of motion for the functional group while permitting easy calculation of the ab initio potential function for any value of q. These calculations included full geometry optimization for all other degrees of freedom which allowed for some coupling between the inversion motion and other modes through both the potential function and the reduced mass. The one-dimensional potential surface obtained by incrementing q was fit by least-squares to an eighth-order polynomial in even powers and substituted into the Schrödinger equation.

$$V(q) = a + bq^2 + cq^4 + dq^6 + eq^8$$

We have implemented Laane's method[42] of obtaining the reduced mass for motion along a generalized coordinate in a FORTRAN program utilizing output from our electronic structure calculations. The value used in each case was determined at the MP2/6-31+G** optimized geometry. Changes in the reduced mass along the inversion coordinate were found to be small. Similar changes in the reduced mass used for the calculations resulted in only small thermodynamic differences and support our assumption of a constant μ for physically reasonable values of q. Solutions to the Schrödinger equation were obtained using the Numerov–Cooley[43] method implemented in a FORTRAN program.[44]

This method shows more basis set consistency for the vibrational transitions and thermodynamic properties when compared to use of the harmonic oscillator vibrational frequencies. Calculated free energy contributions of the inversion mode to formamide and acetamide at the HF/6-31G* and MP2/6-31+G** levels are within 5% of those estimated from experimental data.[45] High-level calculations on ammonia resulted in good agreement with the experimental inversion energy levels[46] and with the results of Campoy et al.[47]

Calculations. The methyl rotational barriers were obtained at the HF/6-31+G** level by incrementing fixed values of the HCNC or HCCO torsional angles. Inversion potential surfaces were obtained at the HF/6-31G* level with the resultant energy

(38) Gordy, W.; Cook, R. L. *Techniques of Chemistry, Vol. XVIII: Microwave Molecular Spectra*; Wiley-Interscience: New York, 1984; pp 569–617.
(39) Atkins, P. W. *Molecular Quantum Mechanics*, 2nd ed; Oxford University Press: New York, 1983.
(40) McQuarrie, D. A. *Quantum Chemistry*; University Science Books: Mill Valley, CA, 1983; pp 262–277. Press, W. H.; Flannery, B. P.; Teukolsky, S. A.; Vetterling, W. T. *Numerical Recipes: The Art of Scientific Computing; FORTRAN Version*; Cambridge University Press: New York, 1990; pp 342–349.
(41) Pitzer, K. S.; Gwinn, W. D. *J. Chem. Phys.* **1942**, *10*, 428.
(42) Laane, J.; Harthcock, M. A. *J. Mol. Spectrosc.* **1982**, *91*, 300.
(43) Cooley, J. W. *Math. Comput.* **1961**, *15*, 363.
(44) Algorithm subroutines written by Dr. Bruce R. Johnson, Rice Quantum Institute.
(45) Hansen, E. L.; Larsen, N. W.; Nicolaisen, F. M. *Chem. Phys. Lett.* **1980**, *69*, 327.
(46) Spirko, V. *J. Mol. Spectrosc.* **1983**, *101*, 30.
(47) Campoy, G.; Palma, A.; Sandoval, L. *Int. J. Quantum Chem. Quantum Chem. Symp.* **1989**, *23*, 355.

levels scaled by 0.893. For both cases, geometry optimization in all other degrees of freedom was carried out using tight convergence (maximum force less than 1.5×10^{-4} H/Bohr or radian).

Acknowledgment. Paul Rablen thanks the National Science Foundation and the American Cyanamid Co. via the Organic Division, ACS, for predoctoral fellowships. We thank Professor Patrick Vaccaro for helpful discussion and the Pittsburgh Supercomputing Center for a grant of computer time. The investigation was supported by a grant from the National Institutes of Health.

Supplementary Material Available: List of experimental rates of methyl group exchange for DMF and DMA at all temperatures measured (from which the values in Table 6 were obtained by least-squares fits to the Eyring equation) (5 pages). This material is contained in many libraries on microfiche, immediately follows this article in the microfilm version of the journal, can be ordered from the ACS, and can be downloaded from the Internet; see any current masthead page for ordering information and Internet access instructions.

JA950073W